Applied Catalysis B: Environmental 180 (2016) 324–329

Contents lists available at ScienceDirect

Applied Catalysis B: Environmental

journal homepage: www.elsevier.com/locate/apcatb

Enhancement of mineralization ability for phenol via synergetic effect of photoelectrocatalysis of g-C_3N_4 film

Fenfen Liang, Yongfa Zhu*

Department of Chemistry, Beijing Key Laboratory for Analytical Methods and Instrumentation, Tsinghua University, Beijing 100084, China

ARTICLE INFO

Article history:
Received 3 February 2015
Received in revised form 24 April 2015
Accepted 6 May 2015
Available online 23 June 2015

Keywords:
Photoelectrocatalysis
Synergetic
g-C_3N_4 film
Mineralization phenol

ABSTRACT

The enhancement of mineralization of phenol via photoelectrocatalytic (PEC) degradation of g-C_3N_4 film under visible light irradiation ($\lambda > 420$ nm) was investigated. The phenol was degraded completely by the g-C_3N_4 with a 2.5 V bias, and 89.3% of the total organic carbon (TOC) was removed, which was 2.4 times the amount achieved using photocatalytic degradation. The synergistic effect of photoelectrocatalysis was proposed to explain the dramatic enhancement. The visible light irradiation was not only able to eliminate the passivation of the g-C_3N_4 electrode for the phenol polymer film at potentials below 1.0 V but also generated a promoting effect of electrocatalytic (EC) oxidation at potentials above 1.0 V. The more active substances, such as OH and O_2^-, could be produced under light irradiation promoted the EC oxidation of phenol and the intermediate products. Simultaneously, the applied bias could reduce the recombination of the photogenerated electron–hole pairs, promote the separation of photogenerated charge carriers, and improve the photocatalytic oxidation efficiency of g-C_3N_4.

1. Introduction

Phenol is an important raw and intermediate chemical material, as well as a common by-product in many industrial enterprises. So it is one of the priority pollutants to be monitored and controlled due to highly toxic and a strong irritant [1]. Traditional methods for the treatment of phenolic wastewater, such as extraction [2], biological treatment [3,4], chemical oxidation [5–7], photocatalytic or electrochemical catalytic oxidation [8–12] have some shortcomings more or less: large energy consumption, incomplete degradation, low mineralization, or high probability of causing secondary pollution. New treatment methods for phenolic wastewater have become an urgent goal for environmental protection workers. Photoelectrocatalysis is an efficient method that was recently proposed that can effectively promote the separation of photogenerated electron-hole pairs, greatly enhancing photocatalytic oxidation performance by exploiting the synergism between photocatalysis and electrocatalysis. Many research results prove that the PEC reaction is more effective at degrading organic pollutants than photocatalysis, phenolic compounds could be completely mineralized into CO_2 and inorganic salts [13–15].

Graphitic carbon nitride (g-C_3N_4) was first reported as a promising photocatalytic material for the decomposition of water to produce hydrogen under visible light ($\lambda > 420$ nm) by the Wang group in 2009 [16,17]. There is increasing concern about g-C_3N_4 in the field of photocatalysis because it is easily prepared, inexpensive, and environmentally benign and has many promising applications [18–24]. To improve the photocatalytic performance of g-C_3N_4, Some modification methods have been reported, such as, copolymerization [25,26], doping [27], texurization [28,29], supermolecular assembly [30], surface heterojunction design [31]. Although g-C_3N_4 has excellent visible light activity, its oxidation capacity is inadequate. It is hard to achieve deep mineralization for phenolic compounds using only photocatalysis [32,33]. Therefore, we consider electrochemical oxidation combined with photocatalysis, which enhanced the intrinsic g-C_3N_4 activity to improve the mineralization of phenolic compounds via a synergistic photoelectric effect.

There have been no reports about the PEC degradation of phenol on g-C_3N_4 under visible light, and the exact mechanism still remains elusive. In this work, g-C_3N_4 thin films were obtained via a simple chemical exfoliation method and were used as the anode in an investigation of the efficiency and mechanism of EC and PEC under different external bias conditions. Additionally, the mechanism of the synergistic effect is also discussed.

* Corresponding author. Fax: +86 10 62787601.
E-mail address: zhuyf@tsinghua.edu.cn (Y. Zhu).

http://dx.doi.org/10.1016/j.apcatb.2015.05.009
0926-3373/

2. Experimental

2.1. Synthesis of g-C_3N_4 Nanosheets.

g-C_3N_4 was prepared by heating Melamine (Tianjin Fuchen Chemical Reagents factory, China) in a muffle furnace for 4 h at 550 °C and kept at this temperature for another 4 h in air. g-C_3N_4 monolayer films were synthesized using the chemical exfoliation method. The as-prepared g-C_3N_4 (2 g) was mixed with 100 mL of H_2SO_4 (98 wt%) in a 250 mL flask and stirred vigorously for 8 h at room temperature. Then, the mixture was slowly poured into 500 mL of water and sonicated for exfoliation. The temperature of the suspension increased rapidly, and the color changed from yellow to white. The resulting suspension was then subjected to 10 min of centrifugation at 2000 rpm to remove any unexfoliated g-C_3N_4. The resulting light white suspension was centrifuged, washed thoroughly with water to remove the residual acid, and then, dried at 80 °C in air overnight. Finally, the resulting products were g-C_3N_4 film powders. The morphology and structure of g-C_3N_4 sample before and after exfoliation were investigated by Transmission electron microscope (TEM), X-ray diffraction (XRD), X-ray photoelectron spectroscopy (XPS), Fourier transform infrared spectroscopy (FTIR) and UV–vis diffuse reflectance spectra (DRS) (Figs. S1 and S2) [34].

2.2. Preparation of the g-C_3N_4 film electrode

The g-C_3N_4 films were prepared on indium–tin oxide (ITO) glass using a dip-coating method [35]. First, 100 mg of the g-C_3N_4 film powders were dispersed in 100 mL of water and, then, treated with ultrasound for 6 h. The ITO glass was immersed in the g-C_3N_4 dispersion, and then, dip coated according to the following process: lifting height: 35 mm, dipping-pulling rate: 50 μm/s, resident time: 30 s, immerse time: 60 s, number of repeated dipping steps: 3 times. The films were dried for 30 min at 80 °C after each dipping. The dispersions were sonicated for 30 min before dipping. The ITO glass was purchased from China Southern Class Co., Ltd. with a thickness of 1.1 mm and a sheet resistance of 15 Ω/□. A typical set of SEM micrographs for g-C_3N_4 film dip-coated onto ITO electrode are shown in Fig. S3. The cross-section analysis of the SEM image was conducted and the thickness of g-C_3N_4 film on the ITO electrode was proved approximately 1 μm (Fig. 3C).

2.3. Photoelectrochemical measurement and degradation

The photoelectrochemical measurements were performed using a CHI 660 B (Shanghai, China) electrochemical workstation and a conventional three-electrode cell system connected with a counter electrode (Pt wire, 70 mm in length with a 0.4 mm diameter), a working electrode (C_3N_4 film, active area of 6 cm^2), and a reference electrode (a saturated calomel electrode, SCE). The working electrode was irradiated with visible light obtained from a 500 W Xe lamp (Institute for Electric Light Sources, Beijing) with 420 nm or UV light obtained from a 15 W germicidal lamp (~90% of the energy output at 254 nm). The average visible light intensity was 0.43 mW cm^{-2}, and the UV light intensity was 0.69 mW cm^{-2} at the position where the film electrodes were placed, which was measured with a radiometer (Photoelectric Instrument Factory Beijing Normal University). An electrolyte solution with a concentration of 0.1 mg L^{-1} Na_2SO_4 was used. The electrochemical impedance spectra (EIS) were performed in the frequency range of 100 kHz–0.05 Hz with an amplitude of the sinusoidal wave of 10 mV. The diagrams of the photocurrent response under visible light and UV light irradiation are shown in Fig.S4.

A phenol solution (100 mL) with an initial concentration of 5 mg L^{-1} was sampled periodically during the reaction. The chromatographic experiments were performed using an HPLC-UV/vis system with an ultraviolet absorbance detector (K 2501) operated at 270 nm and a Venusil XBP-C_{18} (Agela Technologies Inc.) column. A total organic carbon (TOC) analyzer (Multi N/C 2100S TOC/TN, Analytik Jena AG) was used for determination of the mineralization of the phenol solutions.

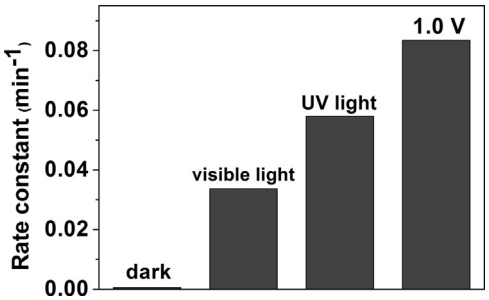

Fig. 1. Apparent rate constants for phenol degradation over g-C_3N_4 film electrode under various conditions in 0.1M Na_2SO_4 solution (visible light, λ > 420 nm; UV lamp, λ = 254 nm; phenol] = 5 ppm).

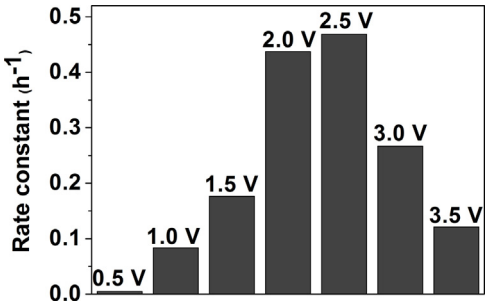

Fig. 2. The rate constants for EC degradation activity of g-C3N4 film electrode for phenol at various potentials in 0.1M Na_2SO_4 solution.

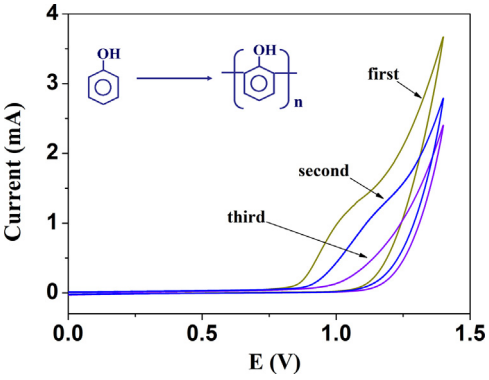

Fig. 3. Cyclic voltammetry scans with the g-C_3N_4 film electrode in a 0.5 M Na_2SO_4 electrolyte with 5 ppm phenol.

3. Results and discussion

3.1. Degradation and mineralization ability of phenol.

3.1.1. Comparison of different processes for phenol degradation

As could be observed from Fig. 1, the concentration of phenol in solution almost did not change in the dark reaction after 5 h. 8.9% of the phenol degradation occurred after 5 h of visible light irradiation, and 10.3% of the degradation occurred after ultraviolet irradiation for 5 h because the conduction and valence bands of g-C_3N_4 generate the photogenerated electrons and holes, respectively, when g-C_3N_4 was excited via light irradiation. The photogenerated holes

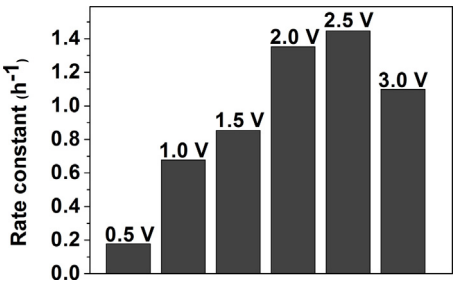

Fig. 4. The comparison of the PEC degradation rate constant *k* of phenol over g-C3N4 at various potentials (visible light, λ > 420 nm, [phenol] = 5 ppm).

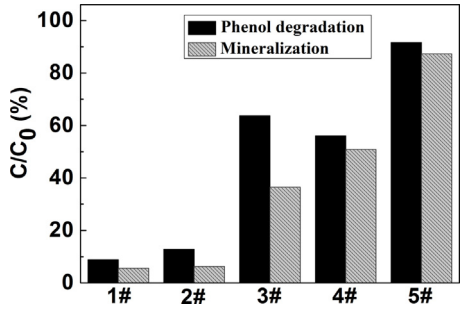

Fig. 5. The degree of the degradation and mineralization of phenol (after reacted for 5 h) at different experimental conditions(1#: Photocatalysis (visible light), 2#: Eletrocatalysis (1.0 V), 3#: Eletrocatalysis (2.5 V), 4#: Photoelectrocatalysis (Visible light + 1.0 V), 5#: Photoelectro-catalysis (visible light + 2.5 V).

could be rapidly transmitted to the surface to directly oxidize phenol, and the photogenerated electrons would produce superoxide or hydroxyl radicals to degrade phenol via a series of reactions. These processes resulted in the rapid and effective separation of photogenerated electrons and holes [36], which showed that g-C_3N_4 has a certain photocatalytic activity, but the catalytic efficiency was low. 12.8% of the phenol was degraded at a bias of 1.0 V in the EC degradation process, which showed that the degree of the EC degradation of phenol was larger than that of the PC degradation. Thus, the application of g-C_3N_4 film in the EC degradation and PEC degradation of phenol was mainly discussed in this paper.

3.1.2. EC and PEC degradation of phenol

Fig. 2 shows the degradation rate constant of the EC degradation of phenol at different biases: 0.5, 1.0, 1.5, 2, 2.5, 3.0 and 3.5 V (The concentration—time graph is shown in Fig. S5A). At a potential of 1.0 V, the EC degradation of phenol was observable, and the degradation rate was increased as a function of the bias potential to 2.5 V, the maximum amount of the phenol degradation reached 63.7% after 5 h at 2.5 V. The phenol degradation fit pseudo first kinetics at bias potentials of 1.0, 2.0, and 2.5 V. Correspondingly, the rate constants were 0.0834, 0.4374, and 0.4686 h^{-1}, respectively (Table S1). Furthermore, the degradation rate of phenol decreased with increasing applied bias. Moreover, nearly no degradation of phenol was observed above 3.5 V after the initial 2 h.

The phenol easily formed on the polymer film on the g-C_3N_4 film electrode, and the electrode became passivated, i.e., unable to catalyze further degradation via the EC process based on the cyclic voltammogram of phenol (Fig. 3). The oxidation peak of phenol appeared nearly 1.0 V, so the phenol polymer film on the surface of the electrode would begin to oxidation reaction and decompose rapidly if the potential was greater than 1.0 V. The electrode could be reactivated and further degradation of phenol would be continued. When the bias voltage was higher than 1.5 V, the water molecules on the surface of the electrode began to electrolyze and produced some strong oxidizing substances, such as •OH radicals and O_2 [37,38]. The oxidation products of phenol could not gather together in polymer film but were further oxidized by these active substances. EC degradation of phenol became faster at higher bias potentials. However, when the bias potential exceeded 3.0 V, oxygen was produced very fast and rapidly reacted with •OH radicals, while the phenolic intermediate products could be oxidized into polymer films on the electrodes and inhibit the degradation of phenol [39]. These results were also consistent with our previous work [35,40].

Generally, the PEC degradation process of organic pollutants in low concentrations also followed pseudo first order kinetics [41]. Under visible light irradiation, the PEC degradation of phenol was determined at potentials of 0.5, 1.0, 1.5, 2.0, 2.5 and 3.0 V. Under different bias voltages, the degradation rate constants of the pseudo first order kinetics of phenol are shown in Fig. 4, (the times variation of the concentration of phenol was given in Fig. S5B). The bias of 0.5 V could significantly increase the PEC degradation of phenol. When the bias voltage was 1.0 V, the degradation of phenol was 56.1% after 5 h, and with increases in the bias, the degradation of the phenol increased. The phenol degraded completely at 2.5 V after 5 h. As the bias increased, the degree of degradation of phenol began to decrease. The degradation rate constants of 0.5, 2.5 and 3.0 V were 0.1782, 1.446 and 1.098 h^{-1}, respectively, (Table S1). Moreover, the phenol degradation rate constant was larger than electric rate constants of EC and PC. (The situation of ultraviolet radiation was the same basically, and the specific data are shown in Fig. S5C.)

During the PEC degradation process, the g-C_3N_4 film electrode did not appear to be passivated, which was because the photogenerated electrons and holes on the g-C_3N_4 film could prevent phenol from formatting a polymer film. Therefore, when the bias potential was low (0.5 V), significant degradation of phenol still occurred. When the bias was 2.5 V, the degradation rate of phenol reached the maximum, which might be because the anode potential could change the space charge layer width of g-C_3N_4, increasing the anodic bias potential, promoting the separation of the photogenerated charge carriers, and reducing the simple recombination of the electrons and holes. At higher bias potentials, the simple recombination rate of electrons and holes was faster. The photogenerated holes were more usable. The hydroxyl free radicals were produced more frequently, which improved the degradation rate of phenol as the applied voltage increased. However, the light intensity was fixed. Thus, the number of photogenerated electrons was certain, so when the bias voltage reached a certain value, the space charge layer was close to the thickness of the film. The electrons and holes basically separated completely, resulting in the best catalytic activity. When the bias potential exceeded 2.5 V, the degradation rate of the phenol layer decreased due to the reallocation of the space charge layer and the Hector Helmholtz layer, reducing the number of photogenerated carriers.

3.1.3. Mineralization of phenol on EC and PEC processes

A total organic carbon analyzer (TOC) was used to evaluate the degree of mineralization of the g-C_3N_4 film electrode under different experimental conditions for phenol. Fig. 5 shows the data for the degradation and mineralization of phenol under different experimental conditions after 5 h. The change in the TOC after PC degradation was the smallest under visible light irradiation. While at biases of 1.0 V and 2.5 V, the changes in the TOC were 6.3% and 36.5% after EC degradation. Combining visible light irradiation with a bias of 1.0 V and PEC resulted in a phenol degradation of 56.1%, and the TOC removal was 47.9%. When the applied voltage was 2.5 V, phenol was degraded completely after 5 h, and the TOC

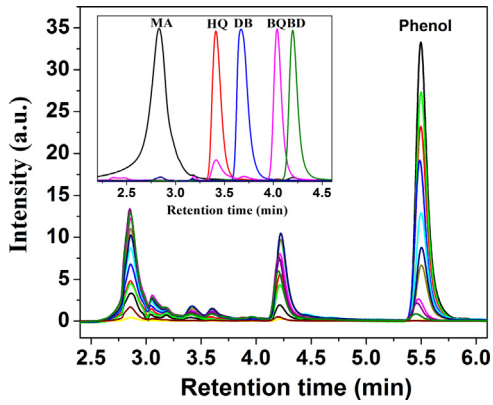

Fig. 6. HPLC spectrums of phenol solution degraded by g-C_3N_4 separately and simultaneously in the PEC process. (BD: *p*-Benzenediol, BQ: Benzoquinone, DB: Dihydroxybenzene, HQ: Hydroquinone, MA: Maleic anhydride).

removal rate reached 89.3%. Therefore, the PEC process could not only improve the degradation rate of phenol but also significantly improve the degree of mineralization. A detailed explanation for these results will be given subsequently.

3.2. Analysis for enhancement of mineralization ability for phenol

3.2.1. Degradation intermediates

High performance liquid chromatography (HPLC) and TOC were used to confirm and quantitatively analyze the intermediate products in the degradation process [42]. The samples for HPLC analysis of phenol solution degraded on EC and PEC process are taken in Fig. 6. There were five common intermediates under both of degradation conditions, and the HPLC spectrums of different standard solution were also shown in the inset of Fig. 6. The intermediate products were mainly aromatic intermediates, such as *p*-benzenediol and benzoquinone. Some of the aromatic intermediates were further oxidized to maleic acid, which was ultimately mineralized into carbon dioxide and water.

Fig. 7A shows that the concentration of phenol decreased and the concentration of the intermediate product of hydroquinone and benzoquinone increased at a bias potential of 2.5 V in the EC process. However, the concentration of the intermediate products changed slowly after 3 h, and further oxidation became slower and mineralization became more difficult. The degradation rate of phenol was 63.7%, while the removal degree of TOC was only 36.5% after 5 h.

Phenol was directly oxidized into a small amount of catechol, hydroquinone and resorcinol via synergistic effect of light irradiation and the applied anodic bias in the PEC process. These substrates could be further oxidized into benzoquinone, but benzoquinone barely accumulated during the reaction, and amounts of maleic acid were detected. Maleic acid was reported to be the ring-open intermediates of phenol and could ultimately mineralize into carbon dioxide and water [43]. Fig. 7B shows that phenol had been completely degraded, and the TOC removal rate had reached 89.3% at a 2.5 V bias under visible light irradiation.

3.2.2. Identification of the active species

The ESR technique could be used to detect radicals in reaction systems [44]. As shown in Fig. 8A, there was no ESR signal in the dark and no obvious ESR signal of $DMPO^-$ •OH adducts with visible light irradiation. However, a gradual evolution of ESR signals for $DMPO^-$ $^•O_2^-$ adducts was observed, suggesting that the molecular O_2 can

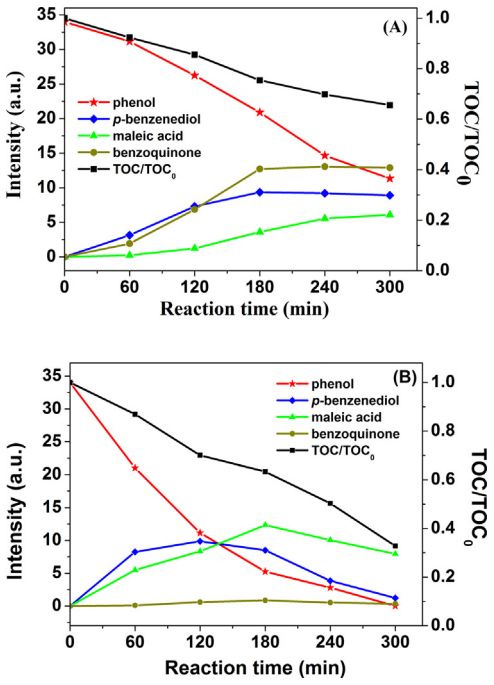

Fig. 7. Distribution of the intermediates and the change of TOC in the EC degradation (A) and PEC degradation (B) process of phenol by C3N4 under visible light irradiation and 2.5 V bias potential.

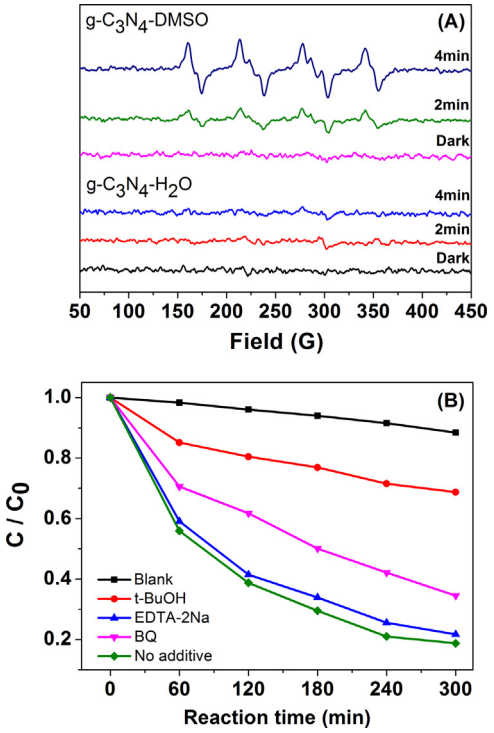

Fig. 8. ESR spectra of g-C_3N_4 film in DMSO solvents and water (A) and The plots of photogenerated carriers trapping (B) on PEC process by C_3N_4 under visible light irradiation and 2.5 V bias potential.

efficiently scavenge photogenerated electrons forming superoxide radical ($^•O_2^-$).

$$O_2 + e^- \rightarrow {}^•O_2^- \quad (1)$$

To confirm the mechanism further, the active species trapping experiment on the PEC degradation of phenol were conducted

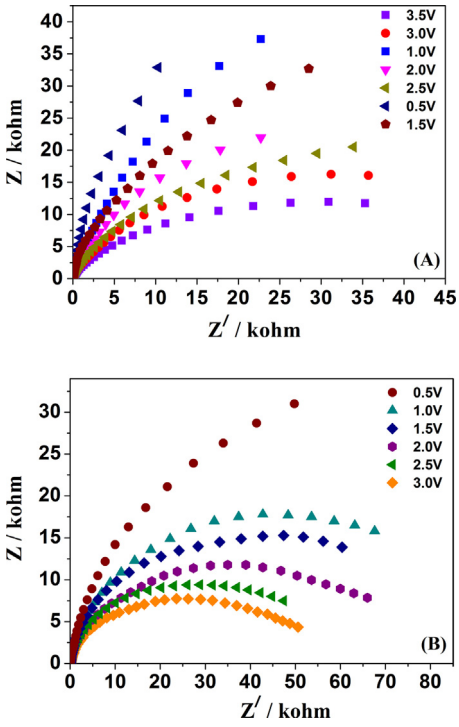

Fig. 9. EIS of EC (A) and PEC (B) degradation of phenol at the g-C_3N_4 film electrode; the amplitude of the sinusoidal wave was 10 mV, and the frequency range of the sinusoidal was 100 kHz to 0.05 Hz.

[45]. Fig. 8B shows the contrast of PEC activity with the addition of hydroxyl radical scavenger (t-BuOH), hole scavenger (EDTA-2Na) and superoxide radical scavenger (1, 4-Benzoquinone, BQ) under visible light irradiation. The PEC activity of g-C_3N_4 decreased slightly by the addition of EDTA-2Na, indicating that the holes were not the main oxidative species for g-C_3N_4 on the PEC process. The PEC activity reduced largely with the addition of BQ, while indicating that superoxide radical are part of oxidative species. The PEC activity was obviously suppressed after the addition of *t*-BuOH, suggesting that hydroxyl radicals •OH were also oxidative species and might directly cause the organic pollutant degradation.

3.3. Mechanism of synergistic effect

Electrochemical impedance spectroscopy (EIS) analysis was used to investigate the photogenerated charge separations process on g-C_3N_4 film electrode. The radius of the circular arc reflected the resistance of the interfacial charge transfer and separation efficiency of the electron-hole pairs [46,47]. Only one radius could be observed on the EIS Nyquist plot shown in Fig. 9A and B, which indicated that the process of EC and PEC degradation of phenol was a simple electrode reaction process. The arc radius decreased gradually as the bias voltage increased. The impedance generated by the Faraday current would decrease due to the increase in the Faraday capacitance constant at the same frequency. Therefore, the reactions on the electrode easily occurred because the energy barrier that the electrode reaction needed to overcome decreased. These data indicated that the increase in the bias potential would improve the catalytic reaction rate and promote the degradation of phenol. Based on the contrast, the radii of the arcs in the EIS Nyquist plot of the PEC process in Fig. 9B were smaller than those of the EC process shown in Fig. 9A. The separation of the photogenerated electron–hole pairs was more effective and the interfacial charge transfer of the electron donor/electron acceptor was faster on the g-C_3N_4 film electrode due to the synergism

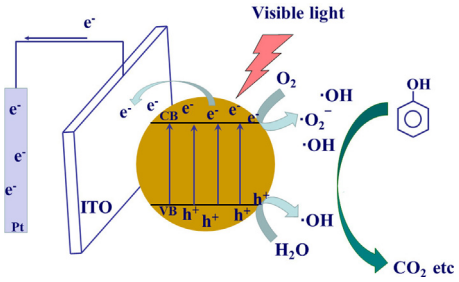

Scheme1. PEC degradation mechanism of phenol by g-C_3N_4 film electrode.

between the light irradiation and the applied anodic bias. (EIS of the phenol degradation of ultraviolet radiation is also shown in Fig. S4D.)

In the process of PEC degradation of phenol, PC and EC would promote and optimize each other, which produced a synergistic effect. The visible light irradiation could not only eliminate the passivation of the electrodes due to phenol polymer film deposition at potentials lower than 1.0 V but could also generate a promoting effect of EC oxidation at potential higher than 1.0 V. Generally, there were two forms of EC degradation of organic compounds: direct and indirect oxidation [48–51]. When the potential was lower than 1.0 V, direct oxidation occurred and the phenol easily formed a polymer film on the g-C_3N_4 film electrodes and the electrodes became passivated and unable to perform further degradation via the EC process. Under visible light irradiation, the photogenerated electrons and holes on the g-C_3N_4 film electrodes could prevent phenol from forming polymer films. When the bias exceeded 1.0 V, the g-C_3N_4 film electrodes mainly adopted indirect EC oxidation degradation of phenol. The anodic current density increased as the bias increased, and then, water could be discharged from the surface of the g-C_3N_4 film electrodes, leading to the evolution of O_2. Under visible light irradiation, O_2 is an acceptor of electrons and might easily produce more active substances, such as $^{\bullet}O_2^-$, H_2O_2 and •OH, which participate in the oxidation of phenol and its intermediate products. The increase in the dissolved oxygen in the solution induced by the electrochemical evolution of oxygen at the anode promoted the production of H_2O_2 at the cathode surface via Eq. (2). However, the H_2O_2 had a lower activity than the •OH radicals and did not efficiently degrade phenol. The •OH radicals could be formed on the basis of the equations (Eqs. (3) and (4)). Thus, the degradation of phenol could be performed via various reactive routes, while promoting the mineralization of the intermediate products.

$$O_2 + 2H^+ + 2e^- \rightarrow H_2O_2 \quad (2)$$

$$H_2O_2 + e^- \rightarrow {}^{\bullet}OH + OH^- \quad (3)$$

$$h^+ + OH^- \rightarrow {}^{\bullet}OH \quad (4)$$

In the meantime, the applied bias improved the photocatalyst efficiency. When a proper bias potential was applied to the C_3N_4 film electrode, the photogenerated electrons would be moved to the counter electrode (Pt electrode) quickly and efficiently via the external circuit under light irradiation. This charge transport process could decrease the recombination of the photogenerated electrons and holes and improve the degradation efficiency, as shown in the PEC degradation process in Scheme 1. The enhancement of holes could not only increase the production of •OH radicals but also prevent the oxidation of intermediates from being reduced. Therefore, the significant synergistic effects between the photocatalytic and electrocatalytic oxidation processes in PEC could improve the degradation of phenol, could significantly improve the efficiency of degradation, and could increase the degree of mineralization of phenol.

3.4. Stability of the C_3N_4 film electrode

The stability of the C_3N_4 film electrodes for the degradation of phenol was also investigated, and the results are shown in Fig. S5D. The PEC degradation process was repeated 5 times using the same electrode, and there were no noticeable changes in the PEC activity of the recycled catalyst after 5 cycles under visible light irradiation combined with a bias potential, indicating that the C_3N_4 film electrode was stable and maintained a similar level of PEC degradation performance after 5 reaction cycles.

4. Conclusions

The g-C_3N_4 thin film was obtained via simple chemical and the g-C_3N_4 film electrode was prepared, which was applied to EC and PEC degradation of phenol. During the PEC degradation process of phenol, PC and EC promote and optimize each other, which produced a synergistic effect. The visible light irradiation could generate a promoting effect of EC oxidation, and in the meantime, the applied bias improved the photocatalyst efficiency. The g-C_3N_4 thin film showed excellent photoelectric catalysis under visible light irradiation. This work provides a simple, efficient and promising technique for the enhancement of the mineralization of phenol.

Acknowledgment

This work was partly supported by National Basic Research Program of China (973 Program) (2013CB632403), National High Technology Research and Development Program of China (2012AA062701), National Natural Science Foundation of China (21437003, 21373121).

Appendix A. Supplementary data

Supplementary data associated with this article can be found, in the online version, at http://dx.doi.org/10.1016/j.apcatb.2015.05.009

References

[1] Phenol, Chemical Week 164 (2002) 31.
[2] W. Kujawski, A. Warszawski, W. Ratajczak, Desalination 163 (2004) 287–296.
[3] H. Temmink, K. Grolle, Bioresour. Technol. 96 (2005) 1683–1689.
[4] H.P. Fang, D.W. Liang, T. Zhang, Water Res. 40 (2006) 427–434.
[5] M. Pérez, F. Torrades, Appl. Catal. B-Environ. 36 (2002) 63–74.
[6] A. Santos, P. Yustos, S. Gomis, Chem. Eng. Sci. 61 (2006) 2457–2467.
[7] A. Alejandre, F. Medina, P. Salagre, Appl. Catal. B-Environ. 18 (1998) 307–315.
[8] A.M. Amat, A. Arques, F. López, M.A. Miranda, Solar Energy 79 (2005) 393–401.
[9] A.V. Emelinea, X. Zhang, T. Murakami, A. Fujishimad, J. Hazard. Mater. 211–212 (2012) 154–160.
[10] H.Y. Jiang, X. Meng, H.X. Dai, J.G. Deng, Y.X. Liu, L. Zhang, Z.X. Zhao, R.Z. Zhang, J. Hazard. Mater. 217–218 (2012) 92–99.
[11] J.L. Boudenne, O. Cerclier, Appl. Catal. A-Gen. 143 (1996) 185–202.
[12] H.Z. Ma, X.H. Zhang, Q.L. Ma, B. Wang, J. Hazard. Mater. 165 (2009) 475–480.
[13] W. Wen, H.J. Zhao, S.Q. Zhang, V. Pires, J. Phys. Chem. C 112 (2008) 3875–3880.
[14] R. Pelegrini, P.P. Zamora, A.R. Andradec, J. Reyes, N. Durána, Appl. Catal. B-Environ. 22 (1999) 83–90.
[15] S.N. Chai, G.H. Zhao, P.Q. Li, Y.Z. Lei, Y.N. Zhang, D.M. Li, J. Phys. Chem. C 115 (2011) 18261–18269.
[16] X.C. Wang, K. Maeda, X.F. Chen, K. Takanabe, K. Domen, Y.D. Hou, X.Z. Fu, M. Antonietti, J. Am. Chem. Soc. 131 (2009) 1680–1681.
[17] X.C. Wang, K. Maeda, A. Thomas, K. Takanabe, G. Xin, J.M. Carlsson, K. Domen, M. Antonietti, Nat. Mater. 8 (2009) 76–80.
[18] G. Liu, P. Niu, C.H. Sun, S.C. Smith, Z.G. Chen, G.Q. Lu, H.M. Cheng, J. Am. Chem. Soc. 132 (2010) 11642–11648.
[19] E.Z. Lee, Y.S. Jun, W.H. Hong, A. Thomas, M.M. Jin, Angew. Chem. Int. Ed. 49 (2010) 9706–9710.
[20] P. Niu, L.L. Zhang, G. Liu, H.M. Cheng, Adv. Funct. Mater. 22 (2012) 4763–4770.
[21] Y.Y. Bu, Z.Y. Chen, J.Q. Yu, W.B. Li, Electrochim. Acta 88 (2013) 294–300.
[22] S.W. Cao, Y.P. Yuan, J. Barber, S.C.J. Loo, C. Xue, Appl. Surf. Sci. 319 (2014) 344–349.
[23] Y.J. Zhong, Z.Q. Wang, J.Y. Feng, S.C. Yan, H.T. Zhang, Z.S. Li, Z.G. Zou, Appl. Surf. Sci. 295 (2014) 253–259.
[24] S.W. Cao, J.G. Yu, J. Phys. Chem. Lett. 5 (2014) 2101–2107.
[25] J.S. Zhang, G.G. Zhang, X.F. Chen, S. Lin, L. Möhlmann, G. Dołęga, G. Lipner, M. Antonietti, S. Blechert, X.C. Wang, Angew. Chem. Int. Ed. 51 (2012) 3183–3187.
[26] Y. Zheng, L.H. Lin, X.J. Ye, F.S. Guo, X.C. Wang, Angew. Chem. Int. Ed. 53 (2014) 11926–11930.
[27] Z.Z. Lin, X.C. Wang, Angew. Chem. Int. Ed. 52 (2013) 1735–1738.
[28] J.S. Zhang, M.W. Zhang, C. Yang, X.C. Wang, Adv. Mater. 26 (2014) 4121–4126.
[29] G.G. Zhang, M.W. Zhang, X.X. Ye, X.Q. Qiu, S. Lin, X.C. Wang, Adv. Mater. 26 (2014) 805–809.
[30] Y.J. Cui, Z.X. Ding, X.Z. Fu, X.C. Wang, Angew. Chem. Int. Ed. 51 (2012) 11814–11818.
[31] J.S. Zhang, M.W. Zhang, R.Q. Sun, X.C. Wang, Angew. Chem. Int. Ed. 51 (2012) 10145–10149.
[32] L.W. J. Xu, R. Zhang, Y.F. Zhu Shi, J. Mater. Chem. A 1 (2013) 14766–14772.
[33] M. Zhang, J. Xu, R.L. Zong, Y.F. Zhu, Appl. Catal. B-Environ. 147 (2014) 229–235.
[34] J.S. Zhang, M.W. Zhang, L.H. Lin, X.C. Wang, Angew. Chem. Int. Ed. 54 (2015), http://dx.doi.org/10.1002/anie.201501001
[35] X. Zhao, Y.F. Zhu, Environ. Sci. Technol. 40 (2006) 3367–3372.
[36] L. Liu, H. Liu, Y.P. Zhao, Y. Wang, Y. Duan, G. Gao, M. Ge, W. Chen, Environ. Sci. Technol. 42 (2008) 2342–2348.
[37] G.W. Muna, N. Tasheva, G.M. Swain, Environ. Sci. Technol. 38 (2004) 3674–3682.
[38] O. Simond, V. Schaller, C. Comninellis, Electrochim. Acta 42 (1997) 2009–2012.
[39] R. Pelegrini, J. Reyes, N. Duran, P.P. Zamora, A.R. De Andrade, J. Appl. Electrochem. 30 (2000) 953–958.
[40] Y.J. Wang, J. Xu, W.Z. Zong, Y.F. Zhu, J. Solid State Chem. 184 (2011) 1433–1438.
[41] R.J. Candal, W.A. Zeltner, M.A. Anderson, Environ. Sci. Technol. 34 (2000) 3443–3451.
[42] Y.F. Liu, Y.Y. Zhu, J. Xu, X.Y. Bai, R.L. Zong, Y.F. Zhu, Appl. Catal. B-Environ. 142–143 (2013) 561–567.
[43] J.A. Zazo, J.A. Casas, A.F. Mohedano, M.A. Gilarranz, J.J. Rodriguez, Environ. Sci. Technol. 39 (2005) 9295–9302.
[44] S.C. Yan, Z.S. Li, Z.G. Zou, Langmuir 26 (2010) 3894–3901.
[45] T.G. Xu, L.W. Zhang, H.Y. Cheng, Y.F. Zhu, Appl. Catal. B-Environ. 101 (2011) 382–387.
[46] J. Lin, R.L. Zong, M. Zhou, Y.F. Zhu, Appl. Catal. B-Environ. 89 (2009) 425–431.
[47] W.H. Leng, Z. Zhang, J.Q. Zhang, C.N. Cao, J. Phys. Chem. B 109 (2005) 15008–15023.
[48] D.J. Rodgers, W. Jedral, N.J. Bunce, Environ. Sci. Technol. 33 (1999) 1453–1457.
[49] X.Y. Lia, Y.H. Cui, Y.J. Feng, Z.M. Xie, J.D. Gu, Water Res. 39 (2005) 1972–1981.
[50] M. Li, C.P. Feng, W.W. Hu, Z.Y. Zhang, N. Sugiura, J. Hazard. Mater. 162 (2009) 455–462.
[51] Y.Z. Zhang, X.Y. Xiong, Y. Han, X.H. Zhang, F. Shen, S.H. Deng, H. Xiao, X.Y. Yang, G. Yang, H. Peng, Chemosphere 88 (2012) 145–154.